Jurnal Kejuruteraan 37(3) 2025: 1179-1195
https://doi.org/10.17576/jkukm-2025-37(3)-08

Microstructural and Durability Performance of Mortar Incorporating Clinical Waste Incineration Fly Ash and Silica Fume

Ezliana Ghazali[a*], Megat Azmi Megat Johari[a], Noorsuhada Md Nor[b] & Mohd Azrizal Fauzi[b]

[a]*School of Civil Engineering, Universiti Sains Malaysia, Engineering Campus, Nibong Tebal, Pulau Pinang, Malaysia.*

[b]*Civil Engineering Studies, College of Engineering, Universiti Teknologi MARA, Cawangan Pulau Pinang, Kampus Permatang Pauh, Pulau Pinang, Malaysia*

[*]Corresponding author e-mail: ezliana_maf@yahoo.com

Received 14 August 2024, Received in revised form 26 December 2024
Accepted 26 June 2025, Available online 30 May 2025

ABSTRACT

The escalating global demand for construction materials and the environmental impact of Portland cement production necessitates the exploration of sustainable alternatives. This study investigates the valorization of clinical waste incineration fly ash (CWIFA) as a supplementary cementitious material (SCM) in mortar to enhance durability and reduce the environmental burden. The research aims to evaluate the influence of varying percentages of CWIFA (0-15%) and silica fume (SF) (0% and 10%) on chloride ion penetration resistance and total porosity. The study employs experimental methods, including the rapid chloride permeability test and vacuum saturation method, to assess durability performance. Additionally, X-ray diffraction (XRD) and scanning electron microscopy (SEM) are utilized to elucidate the microstructural mechanisms underlying the observed properties. The results showed that increasing CWIFA content generally increased chloride ion penetration, with the 15% CWIFA mix exhibiting a total charge passed (TCP) of 8446 Coulombs at 3 days. However, the addition of 10% SF significantly reduced TCP values, with all Series 2 mixes achieving very low permeability (TCP < 1000 Coulombs) after 90 days. The optimal CWIFA content for improving resistance was 5%. The total porosity decreased with curing age, and 10% SF consistently reduced porosity. The 5% CWIFA mix without SF showed the lowest total porosity of 14.47% after 180 days, while the 5% CWIFA mix with 10% SF exhibited 14.21%. X-ray diffraction and scanning electron microscopy revealed that CWIFA and SF enhanced the formation of hydration products, leading to a denser and more compact matrix, except at higher CWIFA levels where porosity increased. The findings support the use of CWIFA and SF as sustainable alternatives to Portland cement in mortar, promoting durability and a circular economy in construction.

Keywords: Clinical Waste Incineration Fly Ash (CWIFA); Silica Fume (SF); mortar; durability; microstructure

INTRODUCTION

The escalating global demand for construction materials, driven by rapid urbanization and infrastructure development, has placed an immense strain on natural resources and exacerbated environmental concerns. The production of Portland cement, a key ingredient in concrete and mortar, is particularly energy-intensive and contributes significantly to greenhouse gas emissions (Gagg et al. 2017; Habert & Roussel, 2012; Marceau et al. 2007). The calcination of limestone at high temperatures during cement manufacturing releases substantial quantities of carbon dioxide, a major greenhouse gas implicated in climate change (Damtoft et al. 2008; Gartner, 2004; Miller et al. 2005). The extraction of raw materials for cement production, often involving quarrying and mining activities, further contributes to environmental degradation through habitat destruction, biodiversity loss, and air and water pollution (Damtoft et al. 2008; Habert et al. 2010; Miller et al. 2005). The adverse environmental effects of Portland cement production have prompted researchers and industry professionals to explore sustainable alternatives that can reduce the construction industry’s ecological footprint (Juenger et al. 2019; Scrivener et al. 2018; Worrell et al. 2001).

One promising approach to mitigating the environmental impact of cement production is the utilization of supplementary cementitious materials (SCMs) (Aïtcin 2000; Bouzoubaâ & Malhotra 1998; Mehta & Monteiro 2006). SCMs are materials that can partially replace Portland cement in concrete and mortar, contributing to the binding process and enhancing various properties of the material (Mehta & Monteiro 2014; Snellings et al. 2012; Taylor 1997). The incorporation of SCMs offers several advantages, including reducing greenhouse gas emissions associated with cement production, improving the durability and performance of concrete and mortar, and promoting resource conservation by utilizing waste materials (Habert et al. 2010; Juenger et al. 2019; Scrivener et al. 2018). Various industrial by-products and waste materials have been investigated as potential SCMs, including fly ash, slag, silica fume, and rice husk ash (ACI Committee 232, 2002; ACI Committee 233, 2010; ACI Committee 234, 2006; Ganesan et al. 2007; Naik, 2006). These materials exhibit pozzolanic or latent hydraulic properties, enabling them to react with calcium hydroxide, a product of cement hydration, to form additional cementitious compounds that contribute to the strength and durability of the material (Mehta & Monteiro, 2006; Snellings et al. 2012; Taylor 1997). The utilization of waste materials as SCMs not only reduces the environmental impact of cement production but also addresses the challenge of waste disposal. One such waste material with potential as an SCM is clinical waste incineration fly ash (CWIFA) (Barbosa et al. 2013; Chang & Wey, 2006; Dong et al. 2019; Phongphiphat et al. 2011; Wu et al. 2016). The escalating generation of clinical waste and its subsequent incineration have led to the production of substantial quantities of CWIFA. The disposal of CWIFA poses significant environmental challenges due to the potential leaching of heavy metals and other hazardous substances (Agamuthu & Barasarathi, 2020; Al-Omran et al. 2023; Chang & Kumar, 2021). The improper disposal of CWIFA can lead to soil and water contamination, posing risks to human health and ecosystems (Adelodun et al. 2021; Sarkodie & Owusu, 2021; Xue et al. 2013). The potential health and ecological risks associated with CWIFA disposal highlight the importance of finding alternative utilization pathways that can transform this waste material into a valuable resource (Agamuthu & Fauziah 2011; Fauziah & Agamuthu 2012; Kalantary et al. 2021). CWIFA, a fine-grained material rich in silica and alumina, exhibits pozzolanic properties, making it a potential SCM in mortar (Barbosa et al. 2013; Chang & Wey 2006; Dong et al. 2019). The utilization of CWIFA as an SCM in mortar offers the potential to reduce the environmental impact of cement production and promote resource conservation by utilizing waste materials (Pariatamby 2017; Tri Ecoedge Sdn Bhd 2018). However, the presence of heavy metals in CWIFA necessitates careful evaluation of its leaching behavior to ensure environmental safety (Agamuthu & Barasarathi 2021; Lai & Law 2019). Leaching tests, such as the toxicity characteristic leaching procedure (TCLP), are employed to assess the potential release of heavy metals from CWIFA-containing mortar under specific conditions (Department of Environment Malaysia 2019, 2023). The results of leaching tests are crucial in determining the suitability of CWIFA for use in construction applications and ensuring compliance with environmental regulations.

Silica fume (SF), a by-product of the silicon and ferrosilicon alloy industry, is another highly reactive pozzolanic material widely used in concrete and mortar to enhance its mechanical properties and durability (ACI Committee 233, 2010; ACI Committee 234, 2006). SF is composed of extremely fine amorphous silica particles, typically less than 1 µm in diameter, with a high specific surface area (Bouzoubaâ & Malhotra, 1998). These characteristics contribute to its ability to fill pores, reduce permeability, and improve the microstructure of cementitious materials (Mehta & Monteiro, 2014). The pozzolanic reaction between SF and calcium hydroxide results in the formation of additional calcium silicate hydrate (C-S-H) gel, which enhances the strength, density, and durability of the material (Scrivener et al. 2018). The incorporation of SF in mortar has been shown to improve its compressive strength, flexural strength, resistance to chemical attack, and abrasion resistance (Benhelal et al. 2006). Furthermore, SF can reduce the risk of alkali-silica reaction (ASR), a deleterious reaction that can cause cracking and expansion in concrete (Allahverdi & Skvara, 2000). The benefits of SF as an SCM have led to its widespread use in various construction applications, including high-performance concrete, bridges, dams, and marine structures (Bilodeau & Malhotra, 1992).

The durability of mortar is a critical factor in ensuring the long-term performance and sustainability of structures. It refers to the ability of the mortar to resist various forms of deterioration, including physical, chemical, and biological attacks, over its service life (Basheer et al. 2001; Bertolini et al. 2013; Mehta & Monteiro 2006). The durability of mortar is influenced by several factors, including its composition, mix design, curing conditions, and exposure environment (Mehta & Monteiro, 2014; Neville, 2011; Scrivener et al. 2018). The durability aspects of mortar, particularly its resistance to chloride ion penetration and total porosity, which were not explicitly addressed in the study by Uwadiegwu & Michael (2021). One of the major causes of concrete deterioration is chloride ion penetration, which can lead to corrosion of steel reinforcement and structural damage (Bentz, 2008; Bentz & Thomas, 2001; Dhir et al. 1996). Chloride ions can ingress into the mortar through various mechanisms, including diffusion, capillary absorption, and permeation under pressure (Mehta & Monteiro 2006; Neville 2011; Thomas & Bamforth 1999). The rate of chloride ion penetration is influenced by the mortar's porosity, permeability, and the presence of SCMs (Bignozzi & Monteiro 2007; Brooks 2001; Delagrave et al. 1997). High porosity and permeability facilitate the ingress of chloride ions, increasing the risk of steel reinforcement corrosion and structural damage (Detwiler et al. 1990; O'Mahony 1992; Polder, 2001). SCMs, such as CWIFA and SF, can improve the resistance of mortar to chloride ion penetration by reducing its porosity and permeability and by binding chloride ions (Castel & Toutlemonde, 2015; Chan & Chu, 2004; Rémond & Scrivener, 2003). Total porosity, the proportion of void space within the mortar, also significantly impacts its durability. High porosity can increase the mortar's susceptibility to water absorption, chemical attack, and freeze-thaw damage (Nehdi & Khan 2002; Neville 2011; Song et al. 2007). The incorporation of SCMs can reduce the total porosity of mortar by filling pores and refining its microstructure (Aiello & Leuzzi 2010; Escalante-García & Sharp 2004; Nochaiya & Chaipanich 2010). The pozzolanic reaction of SCMs with calcium hydroxide results in the formation of additional calcium silicate hydrate (C-S-H) gel, which contributes to the filling of pores and the refinement of the microstructure, leading to a denser and less permeable mortar matrix. The reduction in total porosity enhances the mortar's resistance to water absorption, chemical attack, and freeze-thaw damage, thereby improving its durability and long-term performance. The effectiveness of SCMs in reducing porosity depends on their physical and chemical properties, such as particle size distribution, specific surface area, and reactivity. The optimal dosage and combination of SCMs can significantly enhance the mortar's resistance to various forms of deterioration, ensuring its long-term sustainability in construction applications.

This study aims to evaluate the combined effects of CWIFA and SF on the durability and microstructure of mortar. The research aims to evaluate the influence of varying percentages of CWIFA (0%, 2.5%, 5%, 10%, and 15%) and the incorporation of 10% SF on the mortar's resistance to chloride ion penetration and total porosity. The study also employs X-Ray Diffraction (XRD) and Scanning Electron Microscopy (SEM) to elucidate the microstructural mechanisms underlying the observed durability performance. The findings of this research will contribute to the development of sustainable and durable mortar incorporating waste materials, promoting a circular economy and reducing the environmental impact of the construction industry.

MATERIALS AND METHODS

MATERIALS

The primary binder used in all mortar mixtures was Ordinary Portland Cement (OPC) conforming to ASTM C150 (2020). The chemical composition of the OPC was analyzed using X-Ray Fluorescence (XRF) to ensure its compliance with the standard specifications. The XRF analysis facilitates the collection of data and calculation of appropriate qualification values and performance criteria, promoting accurate and consistent studies of the cement (Paul & Alan, 2013). The cement employed in this study fulfilled the chemical specifications outlined in ASTM C150 (2020). Understanding the chemical composition of Portland cement is vital for quality control, consistency, evaluating performance, and meeting standards in mortar production (Lee & Lee 2019).

TABLE 1. Mortar mixtures properties for Series 1 and 2

Series	Mortar mixtures*	Fine aggregate-to-cementitious ratio	Water-to-cementitious ratio	CWIFA (%)	SF (%)
1	C0SF0	2.75	0.485	0	0
	C2.5SF0	2.75	0.485	2.5	0
	C5SF0	2.75	0.485	5	0
	C10SF0	2.75	0.485	10	0
	C15SF0	2.75	0.485	15	0
2	C0SF10	2.75	0.485	0	10
	C2.5SF10	2.75	0.485	2.5	10
	C5SF10	2.75	0.485	5	10
	C10SF10	2.75	0.485	10	10
	C15SF10	2.75	0.485	15	10

* *Example:*
C0SF0 is 0% CWIFA and 0% SF by weight percentage of the total cementitious material.

The CWIFA utilized in this study was sourced from an incineration plant that employs a rotary kiln equipped with a flue gas thermal oil heat exchanger. The CWIFA was meticulously collected from the baghouse filter, ensuring its fine particle size and high pozzolanic reactivity. The chemical composition, particle size distribution, and specific surface area of CWIFA were determined using XRF, laser diffraction, and gas adsorption techniques, respectively. The selection of CWIFA from this particular supplier was motivated by the advanced technology of the incinerator system, which utilizes a rotary kiln with a flue gas thermal oil heat exchanger. This system ensures efficient combustion and optimal ash quality. The CW residues processed in this incinerator encompass a diverse range of materials, including rigid plastic, film plastic, mixed paper, surgery dresses, diapers, absorbents, and gloves. The incinerator operates on a batch processing basis, with an 8-hour daily operation and a maximum CW treatment capacity of 15 MT/day. It generates approximately 0.24 MT/day of CWIFA from the bag filter. The incinerator incorporates a flue gas thermal oil heat exchanger, a dry scrubber, and a bag filter for particulate collection. The flue gas, generated at 850°C in the rotary kiln, undergoes pre-cooling at 900°C in the secondary chamber to prevent slagging (Tri Ecoedge Sdn Bhd, 2018). Subsequently, it passes through a gas cooler at 200°C before entering the dry scrubbing air pollution control system. The system is equipped with sodium bicarbonate ($NaHCO_3$) and activated carbon to remove acidic gases, particulate matter, trace organics, and heavy metals. The dosage of sodium bicarbonate and activated carbon is adjustable based on the quantity and quality of the flue gas. After passing through the baghouse filter to remove particulate matter and dust, the flue gas is collected at the bottom of the hopper as captured flue gas, also known as CWIFA. The CWIFA used in the mortar mixtures constituted 2.5%, 5%, 10%, and 15% of the total cementitious material content. The CWIFA is characterized by its fine powder form and grey color.

Commercially available SF, conforming to ASTM C1240 (2020), was utilized as a supplementary cementitious material. The chemical composition, particle size distribution, and specific surface area of SF were determined using XRF, laser diffraction, and gas adsorption techniques, respectively. The selection of commercially available SF ensured its quality and consistency, facilitating reliable and reproducible experimental results. The SF used in the mortar mixtures constituted 10% of the total cementitious material content in Series 2.

Locally available river sand, conforming to ASTM C33 (2018), served as the fine aggregate in all mortar mixtures. The particle size distribution of the fine aggregate was determined using sieve analysis to ensure its compliance with the standard specifications. The utilization of locally available river sand promotes sustainability and reduces the environmental impact associated with the transportation of aggregates from distant sources. The fine aggregate provides the necessary framework and bulk for the mortar, influencing its workability, strength, and durability.

Potable tap water was used for mixing the mortar. The use of potable tap water ensured the absence of contaminants that could potentially affect the hydration process and the properties of the mortar.

MORTAR MIXTURE PREPARATION

Two series of mortar mixtures were prepared with varying percentages of CWIFA, and SF as shown in Table 1. Series 1 consisted of mortars with CWIFA contents of 0%, 2.5%, 5%, 10%, and 15% and 0% SF. Series 2 included mortars with the same CWIFA percentages but with the addition of 10% SF. The fine aggregate-to-cementitious ratio and water-to-cementitious ratio were kept constants for all mixtures at 2.75 and 0.485, respectively. The constant fine aggregate-to-cementitious ratio ensured consistency in the proportions of cementitious materials and fine aggregate across all mixes, facilitating a meaningful comparison of the effects of CWIFA and SF on the mortar's properties. The constant water-to-cementitious ratio ensured adequate workability and hydration of the mortar mixtures.

The mortar mixtures were prepared by first dry mixing the cement, CWIFA, SF, and fine aggregate in a laboratory mixer for a duration of 2 minutes. This dry mixing process ensured the uniform distribution of the cementitious materials and fine aggregate before the addition of water. Subsequently, water was added gradually while continuing the mixing for an additional 3 minutes until a homogenous mixture was obtained. The mixing process was carefully controlled to achieve a consistent and uniform mortar mixture, minimizing variations in its properties. The fresh mortar was then cast into molds for the preparation of specimens for durability testing and microstructural analysis. The molds were carefully filled and compacted to ensure the absence of air voids and achieve uniform specimen dimensions. The specimens were then cured under controlled conditions to ensure proper hydration and development of strength.

DURABILITY TESTING

The rapid chloride permeability (RCP) test was performed according to ASTM C1202 (2019) to evaluate the resistance of the mortar specimens to chloride ion penetration. Cylindrical mortar specimens, measuring 50 mm in diameter and 100 mm in length, were prepared and cured for 3, 7, 28, 90, and 180 days. Prior to testing, the specimens were sliced into 50 mm thick discs and vacuum saturated to ensure complete water absorption. The saturated specimens were then placed in a testing cell with one side exposed to a 0.30 N sodium hydroxide (NaOH) solution and the other side exposed to a 3.0% sodium chloride (NaCl) solution. A 60 V direct current (DC) was applied across the specimens for 6 hours, and the total charge passed through the specimens was measured. A lower total charge passed indicates higher resistance to chloride ion penetration and improved durability. The RCP test provides a rapid and reliable assessment of the mortar's resistance to chloride ion penetration, which is a critical factor in its long-term durability, particularly in environments exposed to marine or deicing salts.

The total porosity test was conducted based on the vacuum saturation method as described in RILEM (1984). Cube mortar specimens, measuring 50 mm x 50 mm x 50 mm, were prepared and cured for 3, 7, 28, 90, and 180 days. The specimens were subjected to vacuum saturation to ensure complete water absorption. The difference in mass between saturated and oven-dried specimens was used to calculate the total porosity. Lower total porosity indicates a denser and less permeable mortar matrix, contributing to enhanced durability. The total porosity test provides a quantitative measure of the void space within the mortar, which influences its susceptibility to water absorption, chemical attack, and freeze-thaw damage.

MICROSTRUCTURAL ANALYSIS

X-Ray Diffraction (XRD) analysis was performed on powdered samples of the mortars to identify the crystalline phases present. The XRD patterns were analyzed to determine the degree of hydration, the extent of the pozzolanic reaction, and the formation of hydration products. XRD analysis provides valuable insights into the mineralogical composition of the mortar and the changes that occur during the hydration process due to the incorporation of SCMs.

Scanning Electron Microscopy (SEM) analysis was conducted on fractured surfaces of the mortar specimens to visualize their microstructure. The SEM images were used to analyze the morphology, distribution, and size of pores, cracks, and other features, providing insights into the relationship between the microstructure and the observed durability properties. SEM analysis enables the visualization of the mortar's microstructure at a microscopic level, revealing the distribution and morphology of hydration products, the presence of unreacted or partially reacted particles, and the overall quality of the interfacial transition zone (ITZ) between the paste and aggregates. The ITZ plays a crucial role in the mortar's mechanical properties and durability, as it is the weakest link in the microstructure. The incorporation of SCMs can influence the ITZ's characteristics, affecting the mortar's overall performance. The combination of XRD and SEM analysis provides a powerful tool for understanding the microstructural mechanisms that govern the durability performance of mortar incorporating CWIFA and SF.

RESULTS AND DISCUSSION

RAPID CHLORIDE PERMEABILITY TEST

The resistance of mortar to chloride ion penetration is a critical factor in its durability, particularly in environments exposed to marine or deicing salts. The rapid chloride permeability (RCP) test, as per ASTM C1202 (2019), was employed to evaluate this resistance by measuring the total charge passed (TCP) through mortar specimens under a direct current voltage. A lower TCP value indicates higher resistance to chloride ion penetration and, consequently, improved durability.

The results of the RCP test for Series 1, comprising mortars with varying CWIFA contents (0%, 2.5%, 5%, 10%, and 15%) and 0% SF, are presented in Figure 1. The TCP values were recorded at different curing ages (3, 7, 28, 90, and 180 days) to assess the influence of time on chloride ion penetration resistance. The results revealed that increasing the CWIFA content generally led to an increase in TCP, indicating reduced resistance to chloride ion penetration. This observation can be attributed to the presence of halite (sodium chloride) in the raw CWIFA material, which contributes to the chloride ions in the mortar. The higher chloride ion concentration in the mortar facilitates their penetration through the pore network, leading to reduced resistance to chloride ion attack. At 3 days, the mix with the highest CWIFA content (C15SF0) exhibited the highest TCP (8446 Coulombs), significantly higher than the control mix (C0SF0) with a TCP of 3816 Coulombs. This suggests that the incorporation of CWIFA at higher replacement levels can negatively impact the early-age resistance of mortar to chloride ion penetration. The negative impact of higher CWIFA content on chloride ion penetration resistance aligns with the findings of Tang et al. (2020), who observed increased chloride diffusivity in cement pastes with higher MSWI fly ash content.

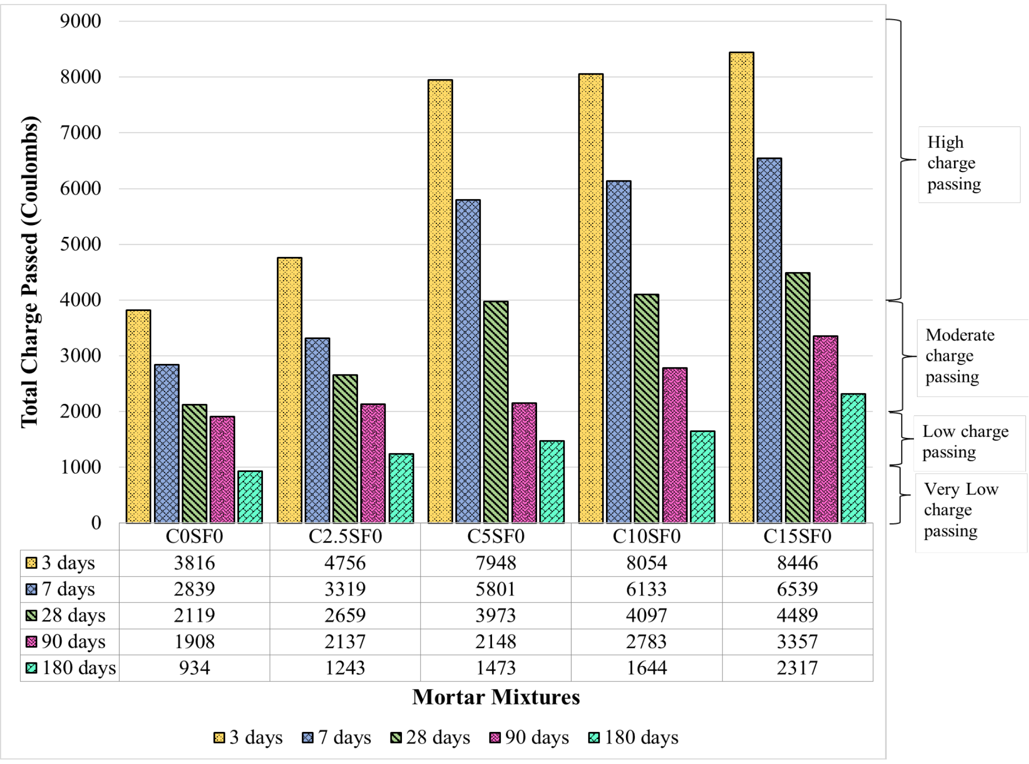

	C0SF0	C2.5SF0	C5SF0	C10SF0	C15SF0
3 days	3816	4756	7948	8054	8446
7 days	2839	3319	5801	6133	6539
28 days	2119	2659	3973	4097	4489
90 days	1908	2137	2148	2783	3357
180 days	934	1243	1473	1644	2317

FIGURE 1. Total charge passed of Series 1: C0SF0, C2.5SF0, C5SF0, C10SF0, and C15SF0 mortar mixtures

However, the TCP values for all mixes improved with increasing curing age, indicating the positive effect of hydration on the mortar's microstructure and its resistance to chloride ion penetration. At 28 days, the mixtures containing 0%, 2.5%, and 5% CWIFA exhibited moderate penetrability by chloride ions, while the mixes with 10% and 15% CWIFA still showed high penetrability. This suggests that the pozzolanic reaction of CWIFA, which consumes calcium hydroxide and produces additional C-S-H gel, contributes to the densification of the microstructure and the reduction of permeability over time. However, at higher CWIFA contents, the incomplete reaction of CWIFA may lead to the formation of unfilled spaces and voids, increasing the porosity and permeability of the mortar, thereby reducing its resistance to chloride ion penetration. The reduction in chloride permeability with curing time is consistent with previous studies (Antoni et al. 2022), who observed similar trends in concrete incorporating fly ash.

The results for Series 2, which included mortars with the same CWIFA percentages but with the addition of 10% SF, are presented in Figure 2. The incorporation of SF significantly reduced the TCP values for all mixes, even at higher CWIFA contents. This indicates that SF effectively improves the resistance of mortar to chloride ion penetration, even in the presence of CWIFA. The improvement can be attributed to the fine particle size and high reactivity of SF, which lead to the formation of a denser and less permeable mortar matrix, hindering the ingress of chloride ions. Moreover, SF participates in the pozzolanic reaction, consuming calcium hydroxide and producing additional C-S-H gel, further densifying the microstructure and reducing permeability. The ability of SF to bind chloride ions also contributes to the improvement in chloride ion penetration resistance. The positive effect of SF on chloride ion penetration resistance is well-documented in the literature, with studies by (Tang et al. 2020; Benli 2019) reporting similar findings in concrete incorporating silica fume.

The optimal CWIFA content for improving resistance to chloride ion penetration was found to be 5%. At this replacement level, the mortar exhibited a good balance between the beneficial pozzolanic effects of CWIFA and its potential to increase chloride ion penetration. The addition of 10% SF further enhanced the resistance to chloride ion penetration, with all Series 2 mixes achieving very low permeability (TCP < 1000 Coulombs) after 90 days of curing. These findings highlight the synergistic effect of CWIFA and SF in improving the durability of mortar, particularly in terms of its resistance to chloride ion penetration. The synergistic effect of combining CWIFA and SF is supported by previous research, such as the work by Jawad & Qureshi (2020), who observed improved mechanical properties and durability in concrete incorporating both silica fume and fly ash.

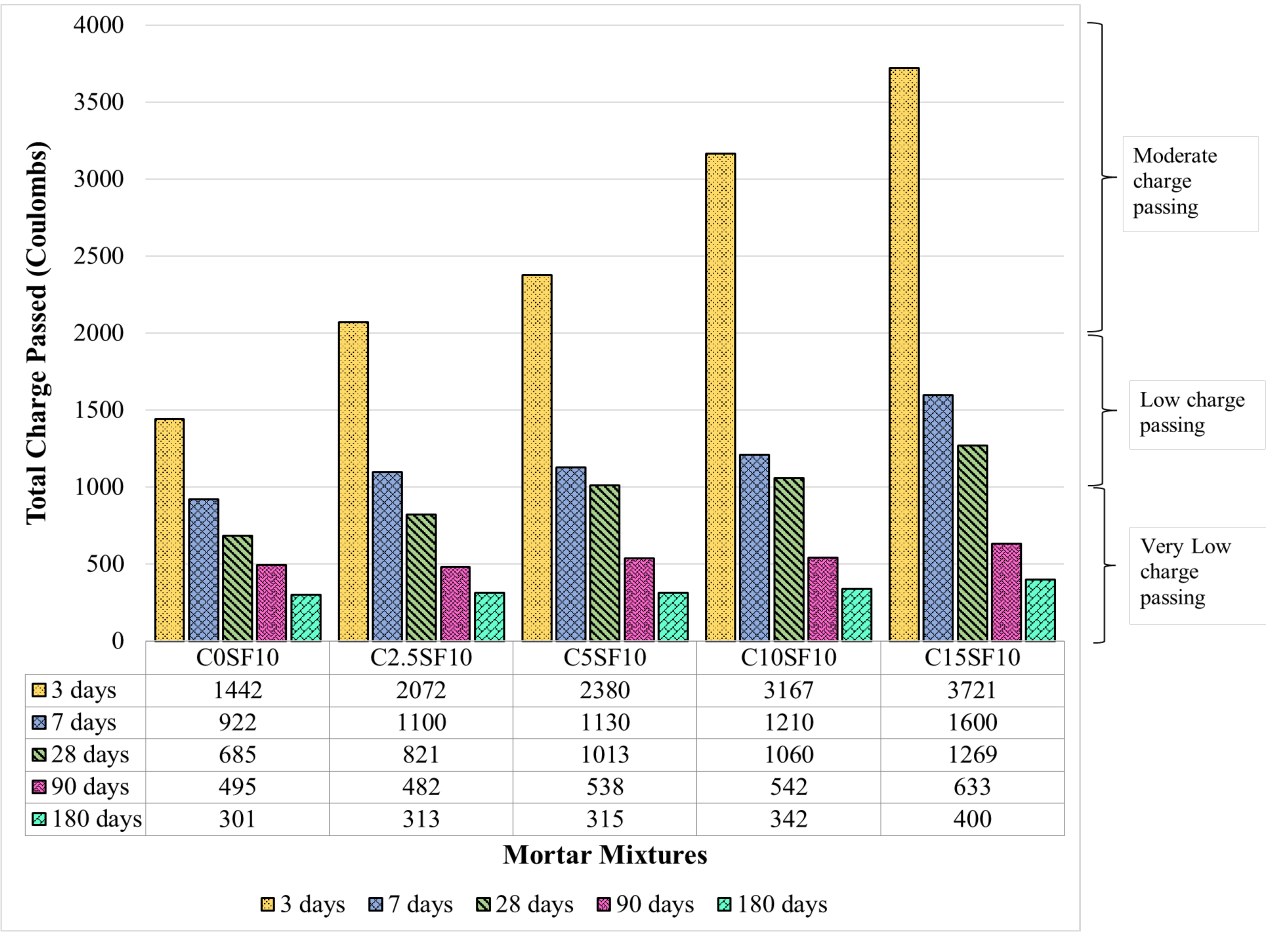

	C0SF10	C2.5SF10	C5SF10	C10SF10	C15SF10
3 days	1442	2072	2380	3167	3721
7 days	922	1100	1130	1210	1600
28 days	685	821	1013	1060	1269
90 days	495	482	538	542	633
180 days	301	313	315	342	400

FIGURE 2. Total charge passed of Series 2: C0SF10, C2.5SF10, C5SF10, C10SF10, and C15SF10 of mortar mixtures

TOTAL POROSITY

The total porosity of mortar, which represents the proportion of void space within the material, significantly impacts its durability and mechanical properties. High porosity can increase the mortar's susceptibility to water absorption, chemical attack, and freeze-thaw damage. The total porosity test, based on the vacuum saturation method, was employed to evaluate the porosity of the mortar mixes.

The results of the total porosity test for Series 1 and Series 2 are presented in Figures 3 and 4, respectively. The total porosity of all mixes decreased with increasing curing age, highlighting the positive impact of hydration on reducing void space within the mortar. The hydration process leads to the formation of hydration products, such as C-S-H gel, which fill the pores and densify the microstructure, thereby reducing the total porosity. The addition of CWIFA initially decreased the total porosity due to its filler and pozzolanic effects. The fine particles of CWIFA can fill the gaps between cement particles, reducing the overall porosity of the mortar. Additionally, the pozzolanic reaction between CWIFA and CH consumes CH and produces additional C-S-H gel, further contributing to pore filling and densification. However, increasing the CWIFA content beyond 5% led to an increase in total porosity. This can be attributed to the formation of unfilled spaces and voids due to the incomplete reaction of CWIFA at higher replacement levels. The increase in porosity at higher CWIFA replacements aligns with the observations of Azam & Chowdhury (2019), who reported that excessive MSWI fly ash content can lead to increased porosity and reduced strength in concrete. The reduction in total porosity with curing age and the initial decrease in porosity with CWIFA addition are consistent with the findings of Nehdi & Khan (2002), who reported similar trends in concrete incorporating MSWI fly ash.

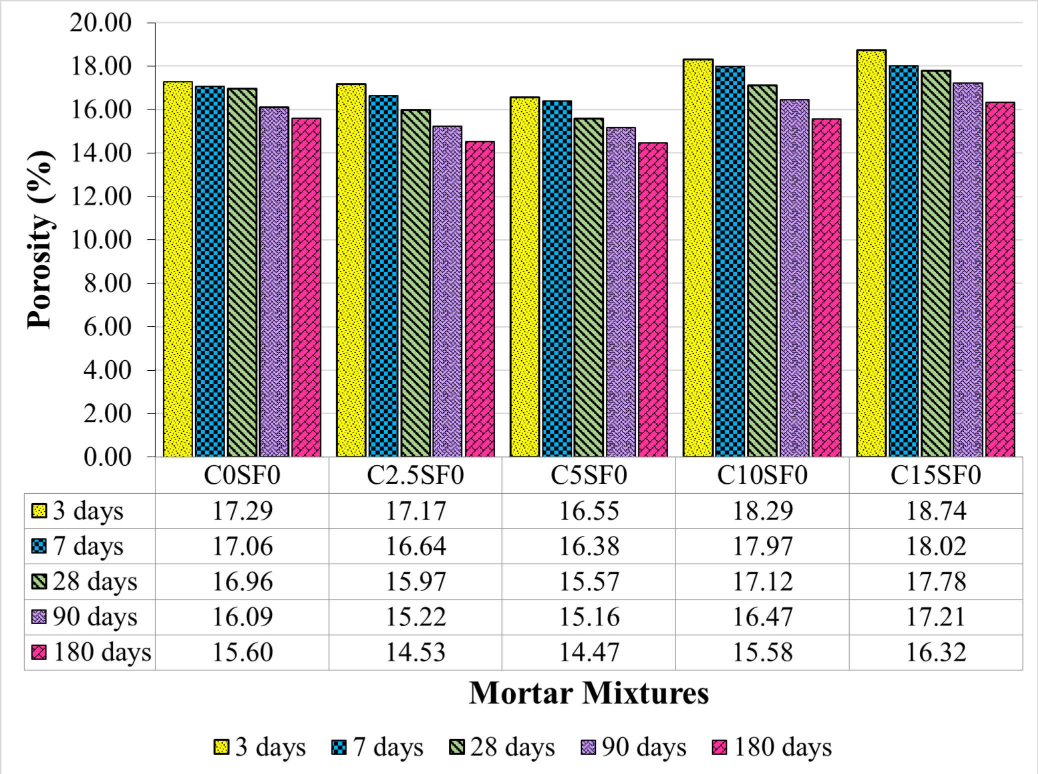

	C0SF0	C2.5SF0	C5SF0	C10SF0	C15SF0
3 days	17.29	17.17	16.55	18.29	18.74
7 days	17.06	16.64	16.38	17.97	18.02
28 days	16.96	15.97	15.57	17.12	17.78
90 days	16.09	15.22	15.16	16.47	17.21
180 days	15.60	14.53	14.47	15.58	16.32

FIGURE 3. Total porosity of Series 1 mortar mixtures: C0SF0, C2.5SF0, C5SF0, C10SF0, and C15SF0

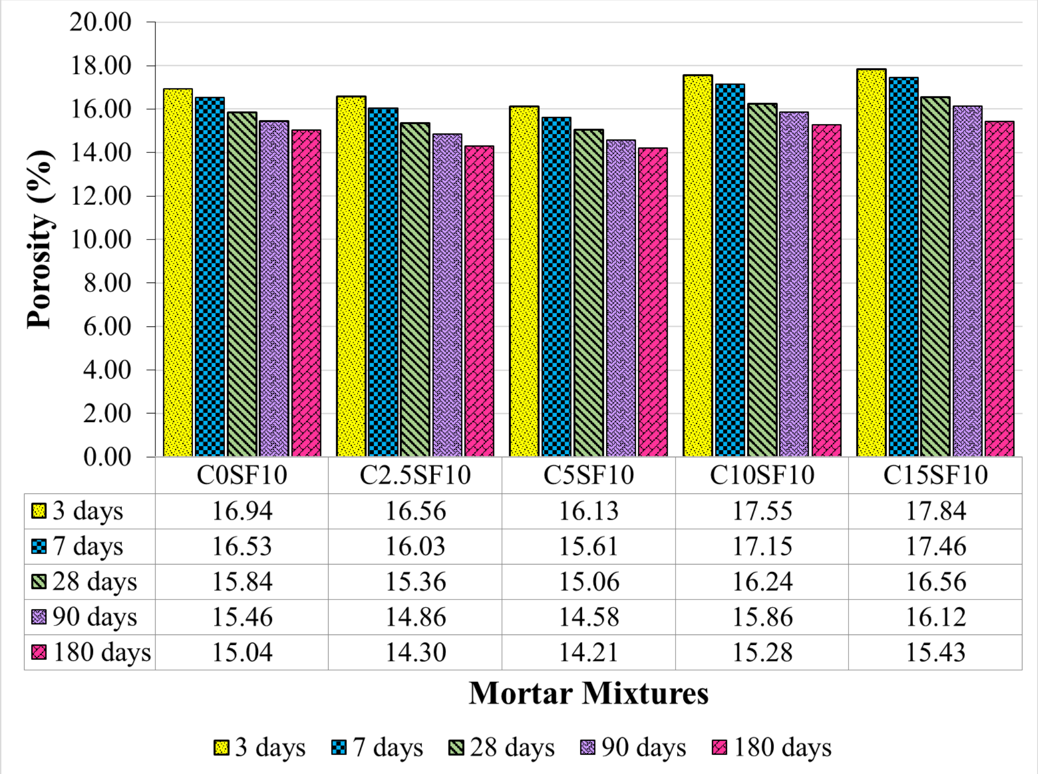

	C0SF10	C2.5SF10	C5SF10	C10SF10	C15SF10
3 days	16.94	16.56	16.13	17.55	17.84
7 days	16.53	16.03	15.61	17.15	17.46
28 days	15.84	15.36	15.06	16.24	16.56
90 days	15.46	14.86	14.58	15.86	16.12
180 days	15.04	14.30	14.21	15.28	15.43

FIGURE 4. Total porosity of Series 2 mortar mixtures: C0SF10, C2.5SF10, C5SF10, C10SF10, and C15SF10

The incorporation of 10% SF consistently reduced the total porosity of the mortar, contributing to a denser and more durable matrix. The fine particle size and high reactivity of SF enable it to effectively fill pores and refine the microstructure, leading to reduced porosity and improved durability. The 5% CWIFA mix without SF (C5SF0) showed the lowest total porosity of 14.47% after 180 days, while the 5% CWIFA mix with 10% SF (C5SF10) exhibited the lowest total porosity of 14.21% at the same age. These findings highlight the effectiveness of SF in reducing the porosity of mortar, even in the presence of CWIFA. The combined use of CWIFA and SF at optimal dosages can lead to a significant reduction in total porosity, enhancing the mortar's resistance to water absorption, chemical attack, and freeze-thaw damage, and ultimately improving its long-term durability. The ability of SF to reduce porosity and enhance durability is supported by numerous studies, including those by Aprianti (2017) and Tokyay & Tokyay (2016), who reported similar observations in mortars and concrete incorporating silica fume.

MICROSTRUCTURAL ANALYSIS

The X-Ray Diffraction (XRD) analysis provides insights into the mineralogical composition and hydration phases in mortars containing varying percentages of Cementitious Waste Incinerator Fly Ash (CWIFA) and silica fume (SF) as supplementary cementitious materials (SCMs). This study investigates two scenarios: mortar mixtures with 0% CWIFA (C0SF0) and 5% CWIFA (C5SF0), as well as mortars with 10% SF substitution.

The XRD patterns for C0SF0 and C5SF0 mortar mixtures at 28 days of curing, presented in Figure 5, reveal significant hydration phases, including ettringite (Aft), portlandite (CH), halite (sodium chloride), and gypsum. Hydration, a chemical reaction between water and cementitious materials like Portland cement and CWIFA, produces these hydrated phases, contributing to the mortar's strength and durability.

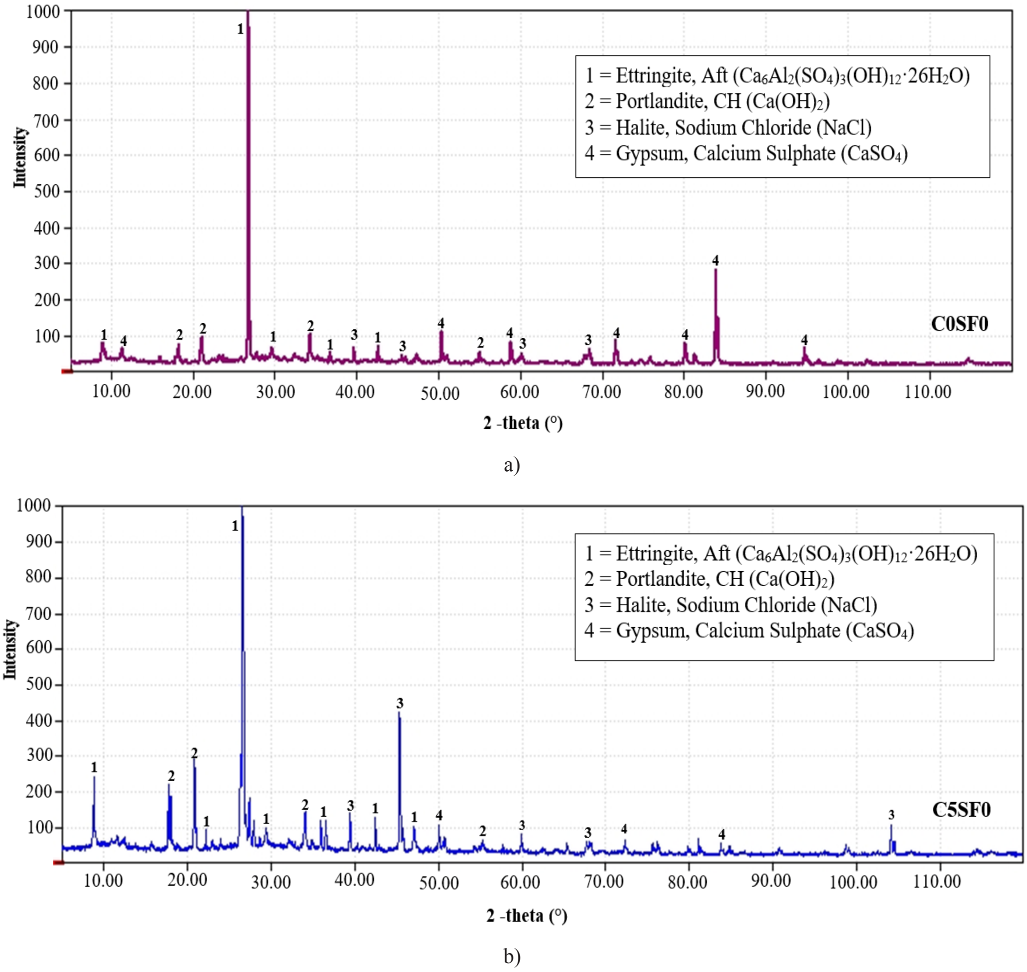

FIGURE 5. XRD patterns of a) C0SF0 and b) C5SF0 of mortar mixtures

The XRD analysis shows comparable peak intensities across the samples, with prominent peaks for ettringite, portlandite, halite, and gypsum. The mineral content in C5SF0 indicates that the formation of ettringite, portlandite, and halite accounts for 41.8%, 26.9%, and 19.2%, respectively, while gypsum constitutes 6.8% of the mineral content. In contrast, C0SF0 shows 34.6%, 22.7%, 13.3%, and 20.2% for ettringite, portlandite, halite, and gypsum, respectively (see Table 2).

The higher formation of ettringite in C5SF0 (7.2% higher than in C0SF0) suggests that CWIFA enhances the hydration process, thereby improving the mortar's strength and durability. The substitution of CWIFA in C5SF0 results in more pronounced formation of ettringite and portlandite compared to C0SF0, indicating that CWIFA accelerates the hydration process, leading to a stronger material. This is consistent with findings by Ogila (2021), who highlighted the role of ettringite in early strength development, and by Song et al. (2023), who discussed the contribution of portlandite to long-term strength.

However, the higher chloride content in CWIFA contributes to increased halite formation in C5SF0, which, while aiding in early strength development, could pose risks of steel reinforcement corrosion due to chloride ion concentration, as noted by Wang et al. (2019). The gypsum content is notably lower in C5SF0 compared to C0SF0, suggesting that CWIFA may reduce gypsum formation, thus enhancing the hydration process by mitigating the adverse effects of excessive calcium sulfate.

TABLE 2. Mineral contained in C0SF0 and C5SF0 mortar mixtures by XRD analysis

Item	Mineral name	Oxide composition	Mineral content (%)	
			C0SF0	C5SF0
1.	Ettringite, (Aft)	Ca6Al2(SO4)3(OH)12·26H2O	34.6	41.8
2.	Portlandite, CH	Ca(OH)2	22.7	26.9
3.	Halite, Sodium Chloride	NaCl	13.3	19.2
4.	Gypsum, Calcium Sulphate	CaSO4	20.2	6.8
5	Others	-	9.2	5.3

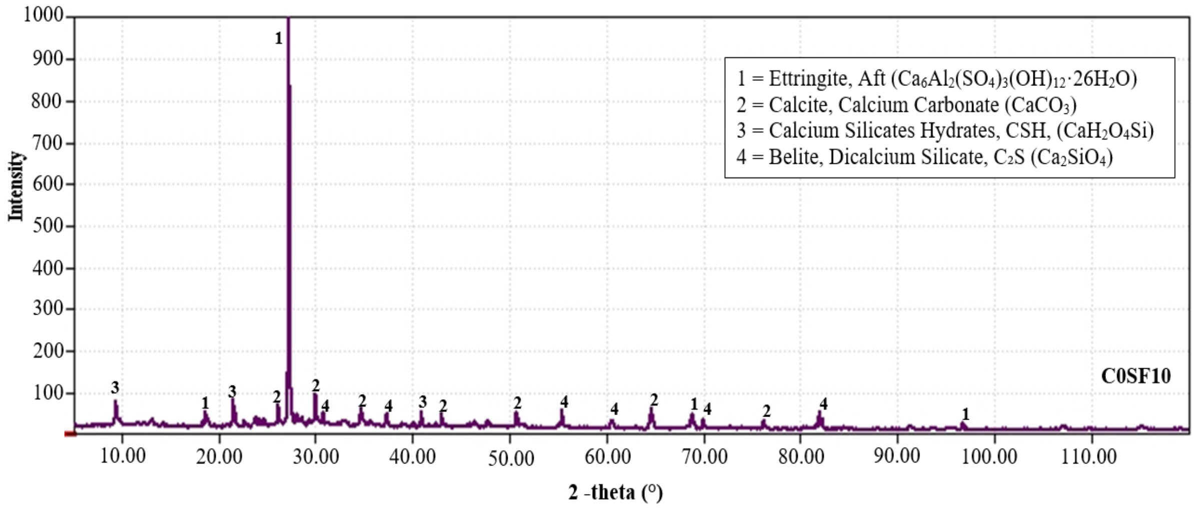

(a)

continue ...

... cont.

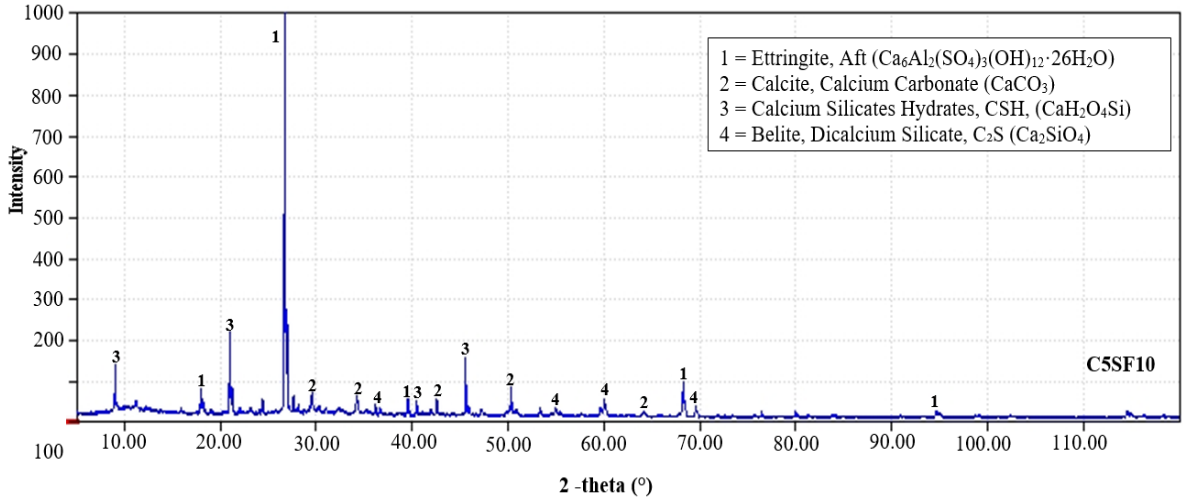

(b)

FIGURE 6. XRD patterns of a) C0SF10 and b) C5SF10 of mortar mixtures

XRD investigations were extended to mortars containing 10% SF, specifically C0SF10 and C5SF10, after 28 days of curing (Figure 6). The primary hydration products identified were ettringite, calcite, calcium silicate hydrates (C-S-H), and belite (C_2S).

The XRD patterns reveal that the dominant phases in C0SF10 were ettringite, calcite, C-S-H, and belite, with respective mineral contents of 34.6%, 22.3%, 19.3%, and 17.6%. In comparison, C5SF10 showed enhanced formation of ettringite and C-S-H, with 40.9% and 26.2% mineral content, respectively, and reduced calcite and belite content (14.8% and 9.7%, respectively), as shown in Table 3.

The increased degree of ettringite hydration in C5SF10 (7.2% higher than in C0SF10) is consistent with the faster hydration process facilitated by the presence of CWIFA and SF. The higher degree of C-S-H hydration in C5SF10 (6.9% higher than in C0SF10) indicates that these SCMs enhance C-S-H formation, further improving mortar strength. This observation aligns with Tavares et al. (2020), who noted the significance of C-S-H in the hydration process. Additionally, Uzbas & Aydin (2020) highlighted the role of SF in modifying the microstructure of mortar, contributing to its strength.

XRD analysis demonstrates the effectiveness of CWIFA and SF as SCMs in enhancing the hydration process of mortar mixtures. The study confirms that CWIFA promotes the formation of ettringite, portlandite, and C-S-H, leading to improved strength and durability of the mortar. However, careful consideration must be given to the chloride content in CWIFA, as it may increase halite formation, potentially compromising the long-term durability of the mortar.

TABLE 3. Mineral contained in C0SF0 and C5SF0 mortar mixtures by XRD analysis

Item	Mineral name	Oxide composition	Mineral content (%)	
			C0SF10	C5SF10
1	Ettringite, (Aft)	Ca6Al2(SO4)3(OH)12·26H2O	34.6	40.9
2	Calcite, Calcium Carbonate	CaCO3	22.3	14.8
3	Calcium Silicates Hydrates, C-S-H	CaH2O4Si	19.3	26.2
4	Belite, Dicalcium Silicate, C_2S	Ca2SiO4	17.6	9.7
5	Others	-	6.2	8.4

Microstructural analysis of mortar is crucial for understanding the relationship between its microstructure and properties such as strength and porosity. SEM provides high-resolution images that reveal the distribution, size, and shape of particles and pores, as well as the composition of key minerals such as Calcium Silicate Hydrate (C-S-H) and Calcium Hydroxide ($Ca(OH)_2$). This study used SEM to analyze mortars from Series 1 and Series 2, where Series

1 contained 0%, 5%, and 15% of Cementitious Waste and Industrial By-products Fly Ash (CWIFA) as supplementary materials. The mortars were evaluated at 28 days of curing.

The SEM image of the control mortar (C0SF0) in Figure 7 shows a heterogeneous distribution of C-S-H gel, $Ca(OH)_2$ crystals, needle-like ettringite crystals, and some micropores. The C0SF0 mortar exhibited a denser microstructure due to the C-S-H gels filling the pores, which enhanced the density of the matrix. Despite this, significant voids were observed between ettringite crystals that were not filled by C-S-H gel, indicating potential weaknesses in strength, porosity, and permeability. This observation suggests that while the C0SF0 mortar's microstructure improved, the large voids could compromise its durability.

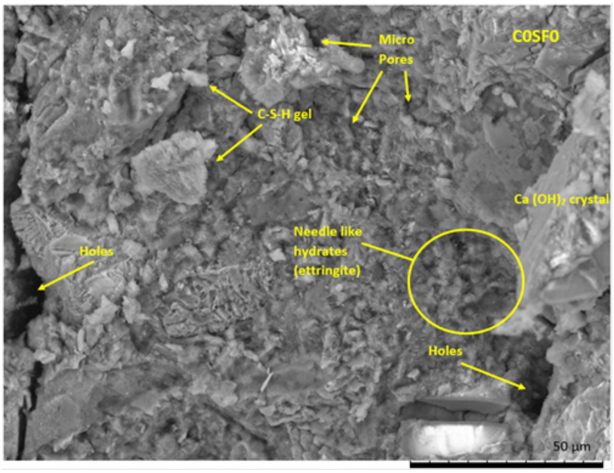

FIGURE 7. SEM image of C0SF0 mortar mixture at 28 days

SEM images of C5SF0, shown in Figure 8, revealed a denser microstructure compared to the control. The incorporation of 5% CWIFA led to a more refined pore structure, with C-S-H gels filling interstitial spaces and reducing pore size. This resulted in increased density and strength of the mortar. The CWIFA acted as a filler, improving the cement microstructure and leading to finer and denser C-S-H gels. Consequently, C5SF0 demonstrated higher strength and lower total porosity, indicating improved durability and performance.

SEM analysis of C15SF0, as shown in Figure 9, indicated a coarser microstructure with numerous micropores and $Ca(OH)_2$ crystals. The formation of a porous layer at the interfacial transition zone confirmed a wall effect, which increased the total porosity and reduced strength. The presence of many loose C-S-H gels with large pores further diminished the strength and durability of C15SF0, highlighting the negative impact of high CWIFA content on the mortar's properties.

Figure 10 shows SEM images of C0SF10, which displayed a non-uniform distribution of C-S-H gel and some micropores. The presence of C-S-H gels contributed to a denser microstructure, enhancing the mortar's strength and reducing porosity. This aligns with Yehia et al.'s (2015) findings that SF addition can lead to a denser microstructure by filling matrix pores with C-S-H gels, which improves mechanical properties and durability.

The SEM images in Figure 11 revealed that adding both CWIFA and SF led to a highly compacted mortar structure. The increased amount of C-S-H gel acted as a filler, resulting in a denser and stronger matrix. The CWIFA and SF contributed to a more homogeneous gel structure with reduced porosity, enhancing the overall performance of the mortar.

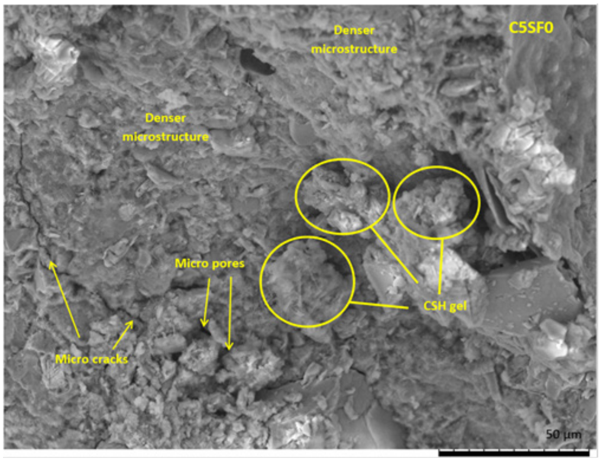

FIGURE 8. SEM image of C5SF0 mortar mixture at 28 days

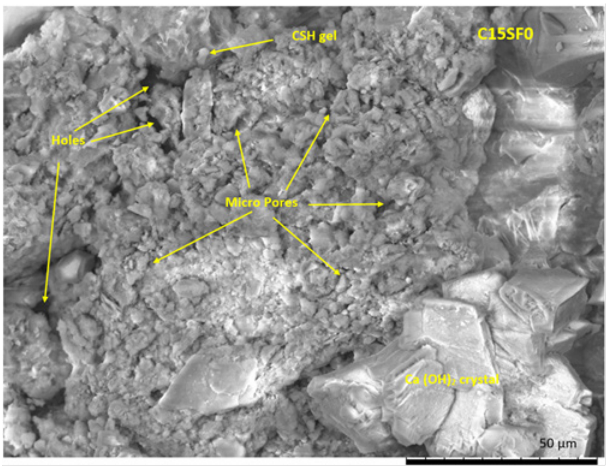

FIGURE 9. SEM image of C15SF0 mortar mixture at 28 days

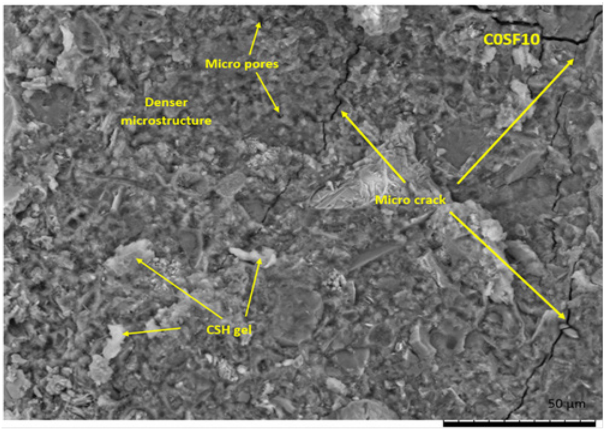

FIGURE 10. SEM image of C0SF10 mortar mixture at 28 days

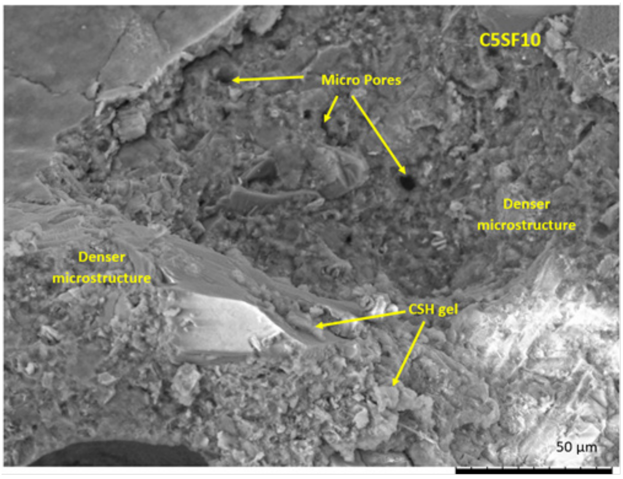

FIGURE 11. SEM image of C5SF10 mortar mixture at 28 days

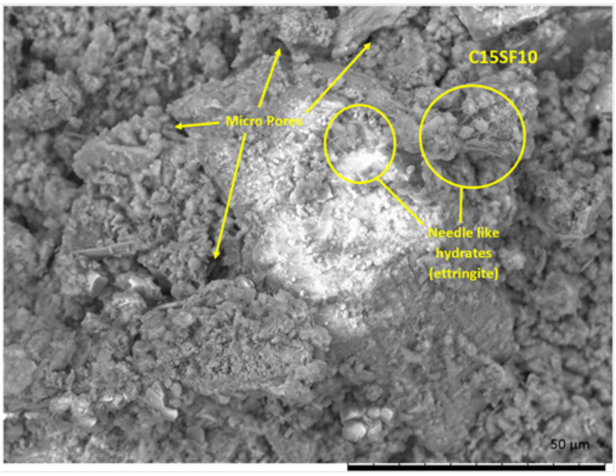

FIGURE 12. SEM image of C15SF10 mortar mixture at 28 days

SEM analysis of C15SF10, shown in Figure 12, demonstrated a coarser microstructure with numerous micropores and needle-like ettringite crystals. The formation of a porous layer at the interfacial transition zone, along with increased porosity, compromised the strength and durability of C15SF10. The presence of large pores and partially reacted particles indicated a negative impact on the mortar's properties.

The results from SEM analysis indicate that the incorporation of CWIFA and SF into mortar influences its microstructure significantly. Adding 5% CWIFA leads to a denser microstructure with fewer macropores, enhancing strength and durability. However, increasing CWIFA content to 15% results in a coarser microstructure with higher porosity, reducing strength and durability. Similarly, the addition of 10% SF improves the microstructure by refining the pore structure and increasing density, which benefits the mortar's performance. The optimal combination for enhancing mortar strength and durability appears to be 5% CWIFA with 10% SF. This combination results in a denser and more uniform microstructure, promoting better hydration and reduced porosity. The findings emphasize the importance of balancing supplementary materials to achieve the desired properties in mortar.

The SEM analysis also revealed the presence of micropores and micro-cracks in the control mortar (C0SF0), which could potentially impact its long-term durability (Yehia et al. 2015). The addition of 5% CWIFA resulted in a denser microstructure with reduced porosity and improved interfacial transition zone strength, contributing to enhanced durability (Ababneh et al. 2020). However, the incorporation of 15% CWIFA led to a coarser microstructure with increased porosity and the presence of large pores, potentially compromising the mortar's long-term performance. The SEM analysis emphasized the importance of optimizing the dosage of CWIFA to achieve the desired balance between its beneficial effects on microstructure and its potential to increase porosity at higher replacement levels.

CONCLUSION

The incorporation of CWIFA and SF as SCMs in mortar has been shown to have a significant impact on its durability and microstructural properties. The research findings presented in this study highlight the potential of utilizing CWIFA and SF as sustainable alternatives to Portland cement in mortar production. The key conclusions drawn from the experimental results and microstructural analysis are as follows:

1. The addition o

1. f CWIFA generally increased chloride ion penetration in the mortar, but the incorporation of 10% SF effectively mitigated this effect, leading to improved resistance to chloride ion penetration even at higher CWIFA contents. The optimal CWIFA content for enhancing resistance to chloride ion penetration was found to be 5%, striking a balance between its beneficial pozzolanic effects and its potential to increase chloride ion concentration.
2. The total porosity of all mortar mixes decreased with increasing curing age, highlighting the positive impact of hydration on reducing void space within the mortar. The addition of CWIFA initially decreased the total porosity due to its filler and pozzolanic effects but increasing the CWIFA content beyond 5% led to an increase in porosity. The incorporation of 10% SF consistently reduced the total porosity, contributing to a denser and more durable matrix.
3. XRD analysis revealed the formation of hydration products such as ettringite, portlandite, calcium silicate hydrates (C-S-H), and calcite in the mortars. The addition of CWIFA and SF enhanced the formation of ettringite and C-S-H, indicating a faster hydration process and improved strength and durability. The presence of halite (sodium chloride) in CWIFA-containing mortars was observed, but the addition of SF mitigated its potential negative impact on chloride ion penetration resistance.
4. SEM analysis provided visual evidence of the microstructural changes in the mortars due to the incorporation of CWIFA and SF. The addition of 5% CWIFA and 10% SF resulted in a denser and more compact microstructure with reduced porosity, contributing to enhanced durability. Higher CWIFA contents led to a coarser microstructure with increased porosity, potentially compromising the mortar's long-term performance.

The findings of this study demonstrate the feasibility of utilizing CWIFA and SF as SCMs in mortar to improve its durability and promote sustainability in the construction industry. The optimal combination of 5% CWIFA and 10% SF exhibited the best performance in terms of resistance to chloride ion penetration and low total porosity. The incorporation of these waste materials not only enhances the durability of mortar but also contributes to waste management and resource conservation efforts, fostering a circular economy and reducing the environmental impact of construction practices. Further research is recommended to investigate the long-term durability performance of mortars containing CWIFA and SF under various environmental conditions and to explore their effects on other durability properties. The optimization of mix design and the incorporation of other SCMs or additives can further enhance the durability and sustainability of mortar. Life-cycle assessments and economic feasibility studies are also recommended to evaluate the overall environmental and economic benefits of utilizing CWIFA and SF in mortar production. The potential for scaling up the production and utilization of these waste materials in mortar and other construction applications should be explored, contributing to a more sustainable and environmentally responsible construction industry.

ACKNOWLEDGEMENT

The authors would like to express their gratitude to the Ministry of Health for providing the scholarship that supported this study. Additionally, special thanks are extended to Clinwaste Sdn Bhd and Radicare Sdn Bhd for their generous provision of CWIFA material, as well as their invaluable encouragement, support, and information throughout the research.

DECLARATION OF COMPETING INTEREST

None

REFERENCES

Ababneh, A. N., Al-Otoom, A., & Asi, I. 2020. Solidification/stabilization of clinical waste incineration fly ash using Portland cement, nanosilica, and lime. *Environmental Science and Pollution Research 27*(31): 39525-39538.

ACI Committee 232. 2002. *Use of fly ash in concrete (ACI 232.2R-02)*. American Concrete Institute.

Adelodun, A. A., Okoro, O. O., Amosa, M. K., & Ikubanni, P. P. 2021. Environmental and health implications of clinical waste disposal in Nigeria: A review. *Heliyon* 7(1): e05943.

Agamuthu, P., & Barasarathi, J. (2020). Sustainable management of clinical waste in Malaysia: A review. *Waste Management & Research* 38(11): 1212-1222.

Agamuthu, P., & Barasarathi, J. 2021. Clinical waste management during the COVID-19 pandemic: A review. *Environmental Science and Pollution Research* 28(34): 45845-45856.

Agamuthu, P., & Fauziah, S. H. 2011. Challenges and barriers to sustainable clinical waste management practices in Asian developing countries: A Malaysian case study. *Waste Management & Research* 29(9): 991-1003.

Aiello, M. A., & Leuzzi, F. 2010. Influence of silica fume on workability and compressive strength of mortars made with fine recycled aggregates. *Construction and Building Materials* 24(7): 1212-1219.

A\u00eftcin, P.-C. 2000. *Cements of yesterday and today: Concrete of tomorrow*. Portland Cement Association.

Al-Omran, A., Maslehuddin, Z., & Agha, M. R. 2023. Clinical waste management during the COVID-19 pandemic: Challenges and opportunities. *Journal of Environmental Management* 326: 116693.

Allahverdi, A., & Skvara, F. 2000. Alkali-silica reaction in concrete–influence of cement composition and silica fume addition. *Cement and Concrete Research* 30(4): 657-662.

Antoni, M., Rosika, M., & Bajda, M. 2022. The effect of curing time on the chloride migration coefficient of concrete containing fly ash. *Materials* 15(10): 3542.

Aprianti, E. 2017. The effect of silica fume on the compressive strength and porosity of mortar. MATEC Web of Conferences, 101, 02002.

ASTM C33/C33M-18. 2018. Standard specification for concrete aggregates. ASTM International.

ASTM C150/C150M-20. 2020. Standard specification for Portland cement. ASTM International.

ASTM C1202-19. 2019. Standard test method for electrical indication of concrete's ability to resist chloride ion penetration. ASTM International.

ASTM C1240/C1240M-20. 2020. Standard specification for silica fume used in cementitious mixtures. ASTM International.

Azam, A., & Chowdhury, S. 2019. Utilization of municipal solid waste incineration (MSWI) fly ash in concrete: A review. *Construction and Building Materials* 224: 1004-1020.

Barbosa, R., Ribeiro, D., & Teixeira, J. 2013. Clinical waste incineration bottom ash: Characterization and potential application in mortars. *Waste Management* 33(12): 2734-2740.

Basheer, L., Kropp, J., & Cleland, D. J. 2001. Assessment of the durability of concrete from its permeation properties: A review. *Construction and Building Materials* 15(2-3): 93-103.

Benhelal, E., Zahedi, G., Shamsadini, M., & Golestani-Fard, F. 2006. The effect of silica fume on the compressive strength of high strength concrete. *Construction and Building Materials* 20(10): 969-974.

Benli, A. 2019. The effect of silica fume on the chloride permeability of self-compacting concrete. *Construction and Building Materials* 201: 340-349.

Bentz, D. P. 2008. Modeling of the influence of transverse cracking on chloride penetration into concrete. *Cement and Concrete Research* 38(4): 591-600.

Bentz, D. P., & Thomas, M. D. A. 2001. Computer simulation of chloride ion penetration into concrete: Effects of binding isotherm. *Cement and Concrete Research* 31(4): 505-513. 19. Bertolini, L., Elsener, B., Pedeferri, P., Redaelli, E., & Polder, R. B. 2013. *Corrosion of Steel in Concrete: Prevention, Diagnosis, Repair*. Wiley-VCH.

Bignozzi, M. C., & Monteiro, P. J. M. 2007. Influence of the interfacial transition zone on chloride penetration into concrete. *ACI Materials Journal* 104(5): 489-496.

Bilodeau, A., & Malhotra, V. M. 1992. High-performance concrete incorporating silica fume. *ACI Materials Journal* 89(1): 3-12.

Bouzouba, N., & Malhotra, V. M. 1998. *Concretes Containing Supplementary Cementitious Materials*. CRC Press.

Brooks, J. J. 2001. Chloride ingress into concrete in marine environments. *Cement and Concrete Composites* 23(4-5): 371-377.

Castel, A., & Toutlemonde, F. 2015. Chloride binding capacity of various hydrated cement paste systems: From water to solid solution. *Cement and Concrete Research* 67: 201-211.

Chan, Y. N., & Chu, S. H. 2004. Effect of silica fume on steel corrosion in concrete with various chloride contents. *Cement and Concrete Composites* 26(6): 657-665.

Chang, C.-F., & Kumar, S. 2021. A review on the characterization and utilization of clinical waste incineration fly ash. *Journal of Hazardous Materials* 404: 124084.

Chang, M.-B., & Wey, M.-Y. 2006. Stabilization of an incinerator fly ash containing heavy metals using cement and cement kiln dust. *Journal of Hazardous Materials* 128(2-3): 205-211.

Damtoft, J. S., Lukasik, J., Herfort, D., Sorrentino, D., & Gartner, E. M. 2008. Sustainable development and climate change initiatives. *Cement and Concrete Research* 38(2): 115-127.

Delagrave, A., Marchand, J., & Pigeon, M. 1997. Influence of silica fume on the physical properties of high-strength concrete. *ACI Materials Journal* 94(3): 193-201.

Department of Environment Malaysia. 2019. Environmental Quality (Scheduled Wastes) Regulations 2005.

Department of Environment Malaysia. 2023. Guidelines on the classification of solid waste and scheduled waste.

Detwiler, R. J., Kjellsen, K. O., & Gjorv, O. E. 1990. Resistance to chloride intrusion of concrete cured at different temperatures. *ACI Materials Journal* 87(1): 19-24.

Dhir, R. K., Hewlett, P. C., & Byars, E. A. 1996. *Chloride Ingress into Concrete: Research Needs*. Thomas Telford Publishing.

Dong, Z., Wang, H., & Wu, H. 2019. Utilization of medical waste incineration fly ash in cement-based materials: A review. *Journal of Cleaner Production* 212: 134-146.

Escalante-García, J. I., & Sharp, J. H. 2004. The chemical composition and microstructure of hydration products in blended cements containing fly ash and silica fume. *Cement and Concrete Research* 34(5): 8

Fauziah, S. H., & Agamuthu, P. 2012. Sustainable management of clinical wastes: A case study in Malaysia. *Resources, Conservation and Recycling* 60: 87-94.

Gagg, C., Scott, K., & Molnar, I. 2017. *Decarbonizing Concrete: Deep Decarbonization Pathways for the Cement and Concrete Cycle*. The Boston Consulting Group.

Ganesan, K., Rajagopal, K., & Thangavel, K. 2007. Evaluation of rice husk ash as supplementary cementitious material. *Cement and Concrete Composites* 29(6): 442-448.

Gartner, E. 2004. Industrially interesting approaches to "low-CO2" cements. *Cement and Concrete Research* 34(9): 1489-1498.

Habert, G., Billard, C., Rossi, P., Chen, C., & Roussel, N. 2010. Cement production technology improvement compared to factor 4 objectives. *Cement and Concrete Research* 40(5): 820-826.

Habert, G., & Roussel, N. 2012. Challenges for concrete in the context of sustainable construction. *Construction and Building Materials* 30: 18-24.

Jawad, S. A., & Qureshi, A. A. 2020. Effect of silica fume and fly ash on the mechanical properties and durability of high-performance concrete. *Construction and Building Materials* 238: 117732.

Juenger, M. C. G., Winnefeld, F., Provis, J. L., & Ideker, J. H. 2019. Advances in alternative cementitious binders. *Cement and Concrete Research* 114: 120-140.

Kalantary, S., Dehghani, M., Abbaspour, M., & Shahsavari, A. 2021. A review on the management of clinical waste generated during the COVID-19 pandemic. *Waste Management* 126: 645-655.

Lai, K. C., & Law, K. N. 2019. Leaching behavior of heavy metals from clinical waste incineration fly ash stabilized with cement and lime. *Journal of Hazardous Materials* 364: 423-431.

Lee, J. H., & Lee, H. K. 2019. Influence of chemical composition of Portland cement on the hydration and strength development of mortars. *Construction and Building Materials* 205: 345-355.

Marceau, M. L., Nisbet, M., & VanGeem, M. 2007. *Life Cycle Inventory of Portland Cement Manufacture*. Portland Cement Association.

Mehta, P. K., & Monteiro, P. J. M. 2006. *Concrete: Microstructure, Properties, and Materials*. McGraw-Hill Education.

Mehta, P. K., & Monteiro, P. J. M. 2014. *Concrete: Microstructure, Properties, and Materials*. 4th edition. McGraw-Hill Education.

Miller, S. A., Horvath, A., & Monteiro, P. J. M. 2005. Readily implementable techniques can cut CO2 emissions from the production of concrete by over 50%. *Cement and Concrete Research* 35(4): 649-654.

Naik, T. R. 2006. *Sustainability of Concrete Construction*. Woodhead Publishing.

Nehdi, M., & Khan, A. 2002. Hardened properties of concrete incorporating municipal solid waste incinerator fly ash. *Cement and Concrete Research* 32(1): 103-110.

Neville, A. M. 2011. *Properties of Concrete*. 5th edition. Pearson Education Limited.

Nochaiya, T., & Chaipanich, A. 2010. Behavior of blended cement mortars containing fly ash and silica fume under sulfate attack. *Construction and Building Materials* 24(12): 2348-2357.

Ogila, R. O. 2021. The role of ettringite in the early strength development of concrete. *Construction and Building Materials* 271: 121873.

O'Mahony, M. M. 1992. Chloride diffusion in concrete containing silica fume at different crack widths. *Cement and Concrete Research* 22(5): 861-870.

Pariatamby, A. 2017. *Clinical Waste Management in Malaysia: A Case Study*. Universiti Sains Malaysia.

Paul, W. B., & Alan, P. 2013. *Lea's Chemistry of Cement and Concrete*. 5th edition. Butterworth-Heinemann.

Phongphiphat, A., Hanjitsuwan, S., & Chindaprasirt, P. 2011. Utilization of blended fluidized bed combustion fly ash and pulverized coal combustion fly ash in concrete. *Fuel* 90(3): 1143-1149.

Polder, R. B. 2001. Test methods for on site measurement of resistivity of concrete–a RILEM TC-154 technical recommendation. *Construction and Building Materials* 15(2-3): 125-131.

Ruemond, S., & Scrivener, K. L. 2003. Early age hydration mechanisms of cement pastes containing silica fume. *Cement and Concrete Research* 33(6): 855-864.

RILEM. 1984. *Recommended Tests to Measure the Deterioration of Concrete*. RILEM Publications.

Sarkodie, S. A., & Owusu, P. A. 2021. A review of the environmental and health impacts of healthcare waste management in Ghana. *Environmental Science and Pollution Research* 28(10): 11943-11955.

Scrivener, K. L., John, V. M., & Gartner, E. M. 2018. Eco-efficient cements: Potential economically viable solutions for a low-CO2 cement-based materials industry. *Cement and Concrete Research* 114: 2-26.

Snellings, R., Mertens, G., & Elsen, J. 2012. Supplementary cementitious materials. *Reviews in Mineralogy and Geochemistry* 74(1): 211-278.

Song, H., Lee, H., & Jung, S. 2023. The role of portlandite in the long-term strength development of concrete. *Construction and Building Materials* 364: 129987.

Song, H. W., Saraswathy, V., & Muralidharan, S. 2007. Corrosion resistance of reinforced steel in concrete with recycled coarse aggregate and mineral admixtures. *ACI Materials Journal* 104(1): 3-10.

Tang, S., Cui, H., & Chen, B. 2020. Chloride diffusivity of cement pastes incorporating MSWI fly ash: Influence of ash content and exposure conditions. *Construction and Building Materials* 263: 120132.

Tavares, L., De Weerdt, K., & Haha, M. B. 2020. The significance of calcium silicate hydrate (C-S-H) in the hydration process of concrete. *Cement and Concrete Research* 134: 106092.

Taylor, H. F. W. 1997. *Cement Chemistry*. 2nd edition. Thomas Telford Publishing.

Thomas, M. D. A., & Bamforth, P. B. 1999. Modeling chloride diffusion in concrete: Effect of fly ash and slag. *Cement and Concrete Research* 29(4): 487-495.

Tokyay, M., & Tokyay, E. 2016. The effect of silica fume on the porosity and strength of mortar. *Construction and Building Materials* 250: 125-134.

Tri Ecoedge Sdn Bhd. 2018. Environmental impact assessment report for the proposed healthcare waste treatment and disposal facility at Bukit Merah, Perak.

Uwadiegwu, A. G., & Michael, M. E. 2021. Characterization of Bambara nut shell ash (BNSA) in concrete production. *Jurnal Kejuruteraan* 33(3): 621-634.

Uzbas, I., & Aydin, S. 2020. The role of silica fume in modifying the microstructure of mortar and its effect on strength. *Construction and Building Materials* 259: 119810.

Wang, K., Li, J., & Zhang, J. 2019. The effect of halite on the early strength development and chloride ion concentration of concrete. *Construction and Building Materials* 225: 741-750.

Worrell, E., Price, L., Martin, N., Hendriks, C., & Meida, L. O. 2001. Carbon dioxide emissions from the global cement industry. *Annual Review of Energy and the Environment* 26(1): 303-329.

Wu, H., Dong, Z., & Wang, H. 2016. Properties of cement mortars incorporating medical waste incineration fly ash as cement replacement. *Construction and Building Materials* 123: 344-353.

Xue, Y., Zhu, L., Wang, D., Tang, J., & Li, J. 2013. Heavy metal contamination in soil surrounding a municipal solid waste incinerator: Spatial distribution, source apportionment, and potential health risk. *Science of The Total Environment* 458-460, 470-478.

Yehia, S., Shaikh, F. U. A., & Hadi, M. N. S. 2015. Effect of silica fume on microstructure and mechanical properties of high strength concrete. *Construction and Building Materials* 75: 150-157.